

(Ag₂TeS₃)₂·A₂S₆ (A = Rb, Cs): Layers of Silver Thiotellurite Intergrown with Alkali-Metal Polysulfides

Sandy L. Nguyen,[†] Joon I. Jang,[‡] John B. Ketterson,[‡] and Mercouri G. Kanatzidis^{*,†,§}

[†]Department of Chemistry, [‡]Department of Physics and Astronomy, Northwestern University, Evanston, Illinois 60208, and [§]Materials Science Division, Argonne National Laboratory, Argonne, Illinois 60439

Received June 4, 2010

The layered compounds RbAg₂TeS₆ and CsAg₂TeS₆ crystallize in the noncentrosymmetric space group *P*6₃*cm*, with *a* = 19.15 Å, *c* = 14.64 Å, and *V* = 4648 Å³ and *a* = 19.41 Å, *c* = 14.84 Å, and *V* = 4839 Å³, respectively. The structures are composed of neutral [Ag₂TeS₃] layers alternating with charge-balanced salt layers containing polysulfide chains of [S₆]²⁻ and alkali-metal ions. RbAg₂TeS₆ and CsAg₂TeS₆ are air- and water-stable, wide-band-gap semiconductors (*E*_g ~ 2.0 eV) exhibiting nonlinear-optical second-harmonic generation.

Chalcogenide compounds can exhibit significant differences in structure, reactivity, and bonding character across the various chalcogen analogues. While sulfide and selenide compounds are often chemically and structurally similar, the telluride analogues are likely to have different structures altogether, e.g., CuQ, NiQ, and PtQ (Q = S, Se, Te).¹ Greater electron delocalization and metallic character of the chalcogen elements from sulfur to tellurium may be correlated with instability in covalent bonding and differences in electronegativity and, of course, size. From a synthetic standpoint, these differences can be exploited to produce compounds containing both elements in different crystallographic sites and even oxidation states,² as opposed to a solid solution (i.e., where S and Te randomly occupy the same crystallographic site). To this end, reactive chalcogenide fluxes containing both S and Te at low temperatures (e.g., 200–400 °C) can

allow for kinetic stabilization of complex building blocks and yield new compounds with unique structural elements. For example, alkali-metal S/Te fluxes can favor the *in situ* oxidation of Te by S–S bonds, depending on the Te/S ratio, and the generation of complex anions, such as the trigonal-pyramidal [TeS₃]²⁻.^{2,3} In the latter, Te is in a formal oxidation state of 4+, making it isoelectronic to [AsS₃]³⁻.⁴

Thiotellurite compounds in the literature have been limited to ternary alkali,⁵ ternary alkaline-earth,⁶ and coinage metal-containing compounds,^{2,3,7} with the exception of the quaternary A₂Mn(TeS₃)₂ (A = Cs, Rb).^{3b} The thiotellurite unit is particularly polarizable because of the presence of a stereochemically active lone pair on the Te atom and the presumed flexibility of the S–Te–S angles.⁸ Compounds containing pyramidal building blocks with stereochemically active lone pairs, such as [AsS₃]³⁻, [IO₃]⁻, and [TeO_x]ⁿ⁻,^{4a,9} that pack into noncentrosymmetric structures have been found to exhibit piezoelectricity, ferroelectricity, and nonlinear optical (NLO) properties.^{8,10}

*To whom correspondence should be addressed. E-mail: m-kanatzidis@northwestern.edu.

- (1) (a) Anderko, K.; Schubert, K. Z. *Metallkd.* **1954**, *45*, 371. (b) Arunsingh Srivastava, O. N.; Dayal, B. *Acta Crystallogr., Sect. B: Struct. Crystallogr. Cryst. Chem.* **1972**, *28*, 635. (c) Baranova, R. V.; Pinskiy, Z. G. *Kristallografiya* **1964**, *9*, 83. (d) Barstad, T.; Gronvold, F.; Rost, E.; Vestersjo, E. *Acta Chem. Scand.* **1966**, *20*, 2865. (e) Bither, T. A.; Bouchard, R. J.; Cloud, W. H.; Donohue, P. C.; Siemons, W. J. *Inorg. Chem.* **1968**, *7*, 2208. (f) Fjellrag, H.; Gronvold, F.; Stolen, S. Z. Z. *Kristallogr.* **1988**, *184*, 111. (g) Fujii, T.; Tanaka, K.; Marumo, F.; Ncda, Y. *Mineral. J.* **1987**, *13*, 448. (h) Furuseh, S.; Kjekshus, A.; Andresen, A. F. *Acta Chem. Scand.* **1969**, *23*, 2325. (i) Gronvold, F.; Haraldsen, H.; Kjekshus, A. *Acta Chem. Scand.* **1960**, *14*, 1879. (j) Kjekshus, A. *Acta Chem. Scand.* **1966**, *20*, 577. (k) Meijer, W. O. J. G. *Am. Mineral.* **1955**, *40*, 693. (l) Nowack, E.; Schwarzenbach, D.; Gonschorek, W.; Hahn, T. Z. *Kristallogr.* **1989**, *186*, 213. (m) Patzak, I. Z. *Metallkd.* **1956**, *47*, 418.
- (2) Zhang, X.; Kanatzidis, M. G. *J. Am. Chem. Soc.* **1994**, *116*, 1890.

- (3) (a) McCarthy, T. J.; Zhang, X.; Kanatzidis, M. G. *Inorg. Chem.* **1993**, *32*, 2944. (b) Zhang, X.; Kanatzidis, M. G. *Inorg. Chem.* **1994**, *33*, 1238. (c) Kanatzidis, M. G.; Park, Y. *Chem. Mater.* **1990**, *2*, 99.
- (4) (a) Bera, T. K.; Jang, J. I.; Ketterson, J. B.; Kanatzidis, M. G. *J. Am. Chem. Soc.* **2008**, *131*, 75. (b) Bera, T. K.; Song, J.-H.; Freeman, A. J.; Jang, J. I.; Ketterson, J. B.; Kanatzidis, M. G. *Angew. Chem.* **2008**, *120*, 7946. (c) Bera, T. K.; Kanatzidis, M. G. *Inorg. Chem.* **2008**, *47*, 7068. (d) Liao, J. H.; Kanatzidis, M. G. *Chem. Mater.* **1993**, *5*, 1561.
- (5) (a) Roth, P.; Schaefer, H.; Weiss, A. Z. *Naturforsch. B: J. Chem. Sci.* **1971**, *26*, 371. (b) Kalyakina, A. V.; Pelyukpashidi, R. I.; Buketov, E. A. *Tr. Khim.-Met. Inst., Akad. Nauk Kaz. SSR* **1972**, *17*, 123. (c) Rumpf, C.; Nather, C.; Bensch, W. *Acta Crystallogr., Sect. C: Cryst. Struct. Commun.* **1999**, *C55*, 1046. (d) Preitschaft, C.; Zabel, M.; Pfitzner, A. Z. *Anorg. Allg. Chem.* **2005**, *631*, 1227. (e) Rieger, F.; Mudring, A.-V. *Chem. Mater.* **2007**, *19*, 221.
- (6) Jumas, J. C.; Ribes, M.; Maurin, M.; Philippot, E. *Acta Crystallogr., Sect. B: Struct. Crystallogr. Cryst. Chem.* **1976**, *B32*, 444.
- (7) (a) Chung, D.-Y.; Huang, S.-P.; Kim, K.-W.; Kanatzidis, M. G. *Inorg. Chem.* **1995**, *34*, 4292. (b) Pfitzner, A.; Zimmerer, S. *Angew. Chem., Int. Ed.* **1997**, *36*, 982.
- (8) Ye, N.; Chen, Q.; Wu, B.; Chen, C. *J. Appl. Phys.* **1998**, *84*, 555.
- (9) (a) Bera, T. K.; Jang, J. I.; Song, J.-H.; Malliakas, C. D.; Freeman, A. J.; Ketterson, J. B.; Kanatzidis, M. G. *J. Am. Chem. Soc.* **2010**, *132*, 3484. (b) Chi, E. O.; Ok, K. M.; Porter, Y.; Halasyamani, P. S. *Chem. Mater.* **2006**, *18*, 2070. (c) Phanon, D.; Gautier-Luneau, I. *Angew. Chem., Int. Ed.* **2007**, *46*, 8488.
- (10) (a) Bergman, J. J. G.; Boyd, G. D.; Ashkin, A.; Kurtz, S. K. *J. Appl. Phys.* **1969**, *40*, 2860. (b) Halasyamani, P. S.; Poeppelmeier, K. R. *Chem. Mater.* **1998**, *10*, 2753.

Here, we report the new compounds $\text{RbAg}_2\text{TeS}_6$ (**1**) and $\text{CsAg}_2\text{TeS}_6$ (**2**) containing $[\text{TeS}_3]^{2-}$ units formed from mixed Te/S polychalcogenide fluxes.¹¹ The structures¹² are composed of neutral $[\text{Ag}_2\text{TeS}_3]$ layers alternating with charge-balanced salt layers of polysulfide chains of $[\text{S}_6]^{2-}$ and alkali-metal ions. In the A/Ag/Te/S (A = Rb, Cs, K) system, a series of compounds with the stoichiometry AAgTeS_3 was obtained in a flux at 300–350 °C,² however, the title compounds were synthesized at 270 °C, a slightly lower temperature. This demonstrates the potential of the flux method for generating novel structures at different temperatures. Evidently, the lower flux temperature stabilized the formation of the polysulfide chain found in the structures; we were unable to synthesize these compounds by direct combination reactions (i.e., without excess polychalcogenide flux).

Optimization of the AAg_2TeS_6 syntheses to yield pure product for material analysis was difficult because of the inherent stability of AAgTeS_3 and Ag_2S as secondary phases. In addition, the lower reaction temperature resulted in inhomogeneities in the melt (presumably because of higher melt viscosity), which have made pure phase synthesis challenging. For example, if the Te/Ag ratio was increased, the reaction products tended to include the already known AAgTeS_3 phase. However, if the Te/Ag ratio is decreased to a point where there was a large excess of Ag, Ag_2S was formed as a secondary phase. In some reactions, both Ag_2S and AAgTeS_3 were formed in addition to AAg_2TeS_6 , indicating melt inhomogeneity. Furthermore, if the temperature was raised above 280 °C, AAgTeS_3 formed in significant yield (>30%). Incidentally, a K-containing analogue was not found for this system. Hence, both the reactant concentration and temperature play a very crucial role in the formation of the AAg_2TeS_6 phases.

Compounds **1** and **2** crystallize in the noncentrosymmetric space group $P6_3cm$ and are composed of intercalated layers of neutral $[\text{Ag}_2\text{TeS}_3]$ and $[\text{A}_2\text{S}_6]$ salt (i.e., two A^+ cations and one $[\text{S}_6]^{2-}$ anion for every two Ag_2TeS_3 units), which are flat and lie perpendicular to the c axis (Figure 1). Although most alkali-metal chalcogenide compounds have anionic frameworks charge-balanced with alkali-metal ions, the unique AAg_2TeS_6 structure type is a composite of two compounds, Ag_2TeS_3 and A_2S_6 , that are capable of existing separately (Figure 1). Hence, a more descriptive formulation for these compounds is $(\text{Ag}_2\text{TeS}_3)_2 \cdot \text{A}_2\text{S}_6$ (A = Rb, Cs).

The Ag atoms are tetrahedrally coordinated by S atoms. The pyramidally coordinated Te atoms of the thiotellurite ion

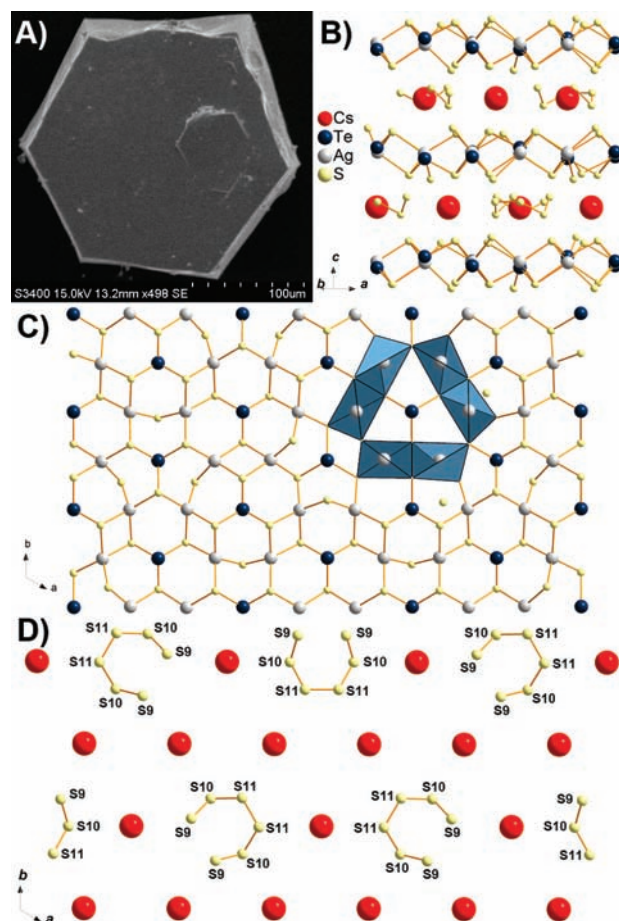


Figure 1. (A) SEM image of the hexagonal crystal and (B) crystal structure view of **2** perpendicular to the $[001]$ direction. (C) $[\text{Ag}_2\text{TeS}_3]$ layer and (D) arrangement of “horseshoe” $[\text{S}_6]^{2-}$ and Cs^+ ions in the $[\text{Cs}_2\text{S}_6]$ layers (S–S distance is ~ 2.02 Å) down the $[001]$ direction.

are found in AAg_2TeS_6 , just as in Ag_2TeS_3 ^{3c,13} and AAgTeS_3 . In **1**, the Te3 atom is disordered, with $\sim 14\%$ of the electron density $0.9167(105)$ Å from the main peak. In AAg_2TeS_6 , because of the presence of the polysulfide salt $[\text{A}_2\text{S}_6]$ layer between $[\text{Ag}_2\text{TeS}_3]$ layers, the AgS_4 tetrahedra share corners and edges within the same layer. This is in contrast to Ag_2TeS_3 , where every Ag atom in a “layer” bonds with one S atom in an adjacent “layer” to complete its tetrahedral coordination, leading to a three-dimensional structure. The hexasulfide ions adopt a horseshoe-like¹⁴ conformation (Figure 1D). The cocrystallized hexasulfide salt moiety in AAg_2TeS_6 effectively breaks up the three-dimensionality of the Ag_2TeS_3 structure. The resulting layered compound has less dense packing of the atoms, decreased electronic band dispersion, and a larger band gap (2.04 eV in AAg_2TeS_6 vs ~ 0.35 eV in Ag_2TeS_3 ;¹⁵ Figure 2A and inset).¹⁶ The difference in the alkali metal is

(11) Preparation of **1**: Amounts of 0.203 g (1 mmol) of Rb_2S , 0.162 g (1.5 mmol) of Ag, 0.064 g (0.5 mmol) of Te, and 0.257 g (8.0 mmol) of S were mixed and loaded into a Pyrex tube. The tube was evacuated to 10^{-3} Torr and flame-sealed. It was then heated to 270 °C in 5 h and held at a constant temperature for 4.5 days, followed by slow cooling to 50 °C at a rate of 4 °C/h. Isolation in *N,N*-dimethylformamide (DMF) resulted in mostly dark-red crystals ($\sim 95\%$) with some black (Ag_2S) and yellow (RbAgTeS_3) secondary material. Preparation of **2**: Amounts of 0.298 g (1 mmol) of Cs_2S , 0.108 g (1 mmol) of Ag, 0.032 g (0.25 mmol) of Te, and 0.257 g (8.0 mmol) of S were mixed and loaded into a Pyrex tube. The tube was sealed and heated according to the same procedure. Isolation in DMF resulted in mostly dark-red crystals ($\sim 95\%$) with some black (Ag_2S) and yellow (CsAgTeS_3) secondary material.

(12) Crystals of **1** are in the space group $P6_3cm$ with $a = 19.146(3)$ Å, $c = 14.642(3)$ Å, and $V = 4648.0(13)$ Å³. Other crystal data: $Z = 18$; $d_c = 3.994$ g/cm³; $\mu = 12.381$ mm⁻¹; total reflections, 22097; independent reflections, 4340; parameters, 165 ($R_{\text{int}} = 0.0735$); $R1 = 0.0769$; $wR2 = 0.1604$; $\text{GOF} = 1.210$. Crystals of **2** are in the space group $P6_3cm$ with $a = 19.410(3)$ Å, $c = 14.829(3)$ Å, and $V = 4838.3(14)$ Å³. Other crystal data: $Z = 18$; $d_c = 4.130$ g/cm³; $\mu = 10.734$ mm⁻¹; total reflections, 35030; independent reflections, 4298; parameters, 160 ($R_{\text{int}} = 0.0472$); $R1 = 0.0754$; $wR2 = 0.1445$; $\text{GOF} = 1.137$.

(13) Pertlik, F. *Monatsh. Chem.* **1997**, *128*, 157.

(14) (a) Müller, A.; Schimanski, J.; Schimanski, U. *Angew. Chem., Int. Ed.* **1984**, *23*, 159. (b) Müller, A.; Zimmermann, M.; Bögge, H. *Angew. Chem., Int. Ed.* **1986**, *25*, 273. (c) Tatsumi, K.; Kawaguchi, H.; Inoue, K.; Tani, K.; Cramer, R. E. *Inorg. Chem.* **1993**, *32*, 4317.

(15) See the Supporting Information.

(16) (a) Axtell, E. A.; Park, Y.; Chondroudis, K.; Kanatzidis, M. G. *J. Am. Chem. Soc.* **1998**, *120*, 124. (b) Axtell, E. A.; Liao, J.-H.; Pikramenou, Z.; Kanatzidis, M. G. *Chem.—Eur. J.* **1996**, *2*, 656. (c) Liao, J. H.; Varotsis, C.; Kanatzidis, M. G. *Inorg. Chem.* **1993**, *32*, 2453. (d) Marking, G. A.; Evain, M.; Petricek, V.; Kanatzidis, M. G. *J. Solid State Chem.* **1998**, *141*, 17. (e) Ruzin, E.; Kracke, A.; Dehnen, S. *Z. Anorg. Allg. Chem.* **2006**, *632*, 1018.

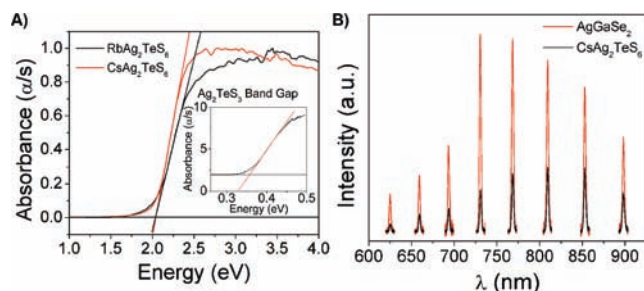


Figure 2. (A) Electronic absorption spectra of **1** and **2** (inset: spectrum of Ag_2TeS_3). (B) SHG intensity (arbitrary units) of **2** relative to that of AgGaSe_2 over a wide wavelength range.

reflected in the increased lattice parameters going from Rb to Cs but not in the band-gap energy (Figure 2) because the dimensionality of the structure is maintained.^{4b}

The S–Te–S angles were found to range from 97.1° to 101.5° .^{2,3,17} The Ag–S bond lengths range from 2.550(7) to 2.671(5) Å, and the shortest Ag–Ag distance is 3.68 Å. The AgS_4 tetrahedra are distorted from the ideal geometry, with the S–Ag–S angles ranging from $89.06(16)^\circ$ to $128.18(18)^\circ$. The large distortion of the angles from the ideal 109.5° tetrahedral angle is due to the side sharing of adjacent AgS_4 tetrahedra; the S–Ag–S angles opposite of the “shared” sides range from $89.06(16)^\circ$ to $91.08(14)^\circ$. In $[\text{S}_6]^{2-}$ [atoms S9–S11], the bond length is ~ 2.02 Å, as expected. The S–S–S angles of the $[\text{S}_6]^{2-}$ chain range from 106.1° to 119.1° .

Differential thermal analysis (DTA) revealed that **2** exhibits a melting point endotherm at 311°C and a crystallization exotherm at 310°C . However, a second cycle of heating and cooling shows incongruent melting because the melting and crystallization peaks are shifted to lower temperatures (305 and 300°C , respectively). After DTA, a dark-red-brown ingot was obtained. Similar results were found for **1**. Powder X-ray diffraction (XRD) of the samples after DTA demonstrated that Ag_2TeS_3 is formed during decomposition, presumably with Cs_2S_6 .¹⁸ Interestingly, the melting point of **2** is between that of Ag_2TeS_3 (358°C) and that of Cs_2S_6 ($\sim 182^\circ\text{C}$).¹⁹

UV–visible electronic absorption spectroscopy revealed a band gap of 2.04 eV for **1** and **2** (Figure 2A). Raman spectroscopy of **1**, **2**, and Ag_2TeS_3 was performed with difficulty because extended exposure to the laser beam during measurement resulted in partial damage to the samples.²⁰ The compounds share several related peaks in the far- to mid-IR region. The Te–S vibrations of the $[\text{TeS}_3]^{2-}$ units can be seen in the Raman spectrum between 316 and 374 cm^{-1} , with the values shifted to slightly lower frequencies in Ag_2TeS_3 . The peaks near 220 cm^{-1} and below are attributed to S–Te–S bending modes.² In **1** and **2**, the two peaks seen between 398 and 425 cm^{-1} are attributed to Ag–S and S–S vibrations in

the $[\text{S}_6]^{2-}$ polysulfide chains.²¹ The spectra also share a strong peak between 460 and 472 cm^{-1} , which is also in the range of S–S vibrations.

Because of the centrosymmetry of the $[\text{Ag}_2\text{TeS}_3]$ layers and the disorder of the S atoms in the polysulfide chains, there were difficulties deciding between centrosymmetric and non-centrosymmetric space groups. A second-harmonic-generation (SHG) measurement was performed to assess the structure symmetry and properly refine the crystal structures. The relative SHG signal intensities of **2** ($45\text{--}63\text{ }\mu\text{m}$ particle size) compared with those of AgGaSe_2 , a benchmark SHG material with NLO properties in the IR region,²² under similar conditions were measured at different wavelengths ($600\text{--}903\text{ nm}$) to analyze the symmetry and NLO properties (Figure 2B). The SHG results confirmed that the compounds adopt a noncentrosymmetric space group. The relative weakness of the SHG intensity compared to that of AgGaSe_2 suggests that the noncentrosymmetry results only from the conformation and orientation of the polysulfide chains because the neutral layers of Ag_2TeS_3 are centrosymmetric. Phase-matching experiments using differently sized particles of **2** ($10\text{--}137.5\text{ }\mu\text{m}$) indicated that the material is type I phase-matchable.²³

The AAg_2TeS_6 ($A = \text{Rb}, \text{Cs}$) compounds have a unique structure featuring layers of $[\text{Ag}_2\text{TeS}_3]$ intercalated by layers of $[\text{A}_2\text{S}_6]$. This is very different from most solid-state compounds, which are generally composed of an anionic or cationic network with counterions in the interstices. Also, technically the compounds are unusual members of the broader silver polychalcogenide family $[\text{Ag}_x\text{Q}_y]^{n-}$ as they contain a fraction of their Q atoms in a highly oxidized state.²⁴ These materials also demonstrate phase-matchable SHG characteristics.¹⁴ The NLO properties are thought to arise from the noncentrosymmetric orientation of the polysulfide chains between the centrosymmetric layers of $[\text{Ag}_2\text{TeS}_3]$, indicating that even small subtleties in the structure can affect the functional properties of materials. Stabilization of the thiotellurite and polysulfide chain building units in these compounds by tuning the flux temperature contributes to our understanding of flux basicity and growth mechanisms.

Acknowledgment. Financial support for this work was received from National Science Foundation Grant DMR-0801855. SEM/EDS analyses were performed at the EPIC facility of the NUANCE Center at Northwestern University (NU), supported by NSF-NSEC, NSF-MRSEC, the Keck Foundation, the State of Illinois, and NU.

Supporting Information Available: X-ray crystallographic files (CIF), structural information tables, and experimental data (powder XRD, DTA, IR, Raman, and phase-matching). This material is available free of charge via the Internet at <http://pubs.acs.org>.

(17) Pfitzner, A. *Inorg. Chem.* **1998**, *37*, 5164.

(18) See the Supporting Information.

(19) Sangster, J.; Pelton, A. D. *J. Phase Equilib.* **1997**, *18*, 78.

(20) See the Supporting Information.

(21) Ziemann, H.; Buss, W. *Z. Anorg. Allg. Chem.* **1979**, *455*, 69.

(22) Bordui, P. F.; Fejer, M. M. *Annu. Rev. Mater. Sci.* **1993**, *23*, 321.

(23) Paschotta, R. In *Encyclopedia of Laser Physics and Technology*; Paschotta, R., Ed.; Wiley-VCH: Berlin, 2008; Vol. *XII*, p 844.

(24) (a) Kanatzidis, M. G.; Huang, S. P. *Inorg. Chem.* **1989**, *28*, 4667. (b) Kanatzidis, M. G.; Huang, S. P. *J. Am. Chem. Soc.* **1989**, *111*, 760. (c) Huang, S. P.; Kanatzidis, M. G. *Inorg. Chem.* **1991**, *30*, 1455.